Realization of Ru–C Eutectic Point for Evaluation of W–Re and IrRh/Ir Thermocouples

H. Ogura · S. Masuyama · M. Izuchi · K. Yamazawa · M. Arai

Abstract Tungsten–rhenium (W–Re) thermocouples are widely used in industry for measurements at high temperatures, up to 2000 °C. Since the electromotive force (emf) of a W–Re thermocouple is known to change during exposure at high temperatures, evaluation of the emf stability is essential for measuring temperature precisely and for realizing precise temperature control used to ensure the quality of products subject to annealing processes. To evaluate precisely the thermoelectric stability around 2000 °C, two Ru–C (1953 °C) cells (crucible and Ru–C eutectic alloy) were constructed in our laboratory. The key feature of the cells is that their dimensions are large to ensure there is sufficient immersion available to evaluate the homogeneity characteristics of the thermocouples. By using one of the Ru–C cells, the drift and inhomogeneity of Type C (tungsten–5 % rhenium vs tungsten–26 % rhenium) thermocouples during an exposure to high temperature around 2000 °C were evaluated. Furthermore, to explore possible applications of the eutectic point to other types of high-temperature thermocouples, the drift of an IrRh/Ir thermocouple (iridium–40 % rhodium vs iridium) was also evaluated using another Ru–C cell. The tests with W–Re and IrRh/Ir thermocouples demonstrate that the newly developed Ru–C cells can be used to successfully realize melting plateaux repeatedly. This enables the long-term drift measurements essential for the evaluation and improvement of high-temperature thermocouples. The results obtained in this study will also be useful for evaluating the uncertainty of thermocouple calibrations at around 2000 °C.

Keywords Drift · Inhomogeneity · IrRh/Ir thermocouple · Ru–C eutectic point · Type C thermocouple · W–Re thermocouple

H. Ogura (✉) · S. Masuyama · M. Izuchi · K. Yamazawa · M. Arai
National Metrology Institute of Japan, National Institute of Advanced Industrial Science
and Technology (NMIJ, AIST), 1-1-1 Umezono, Tsukuba, Ibaraki, Japan
e-mail: h.ogura@aist.go.jp

1 Introduction

In industry, high-temperature thermocouples are widely used for realizing precise temperature control applied to maintain the quality of products that are subject to an annealing process at high temperature up to 2000 °C. Tungsten–rhenium (W–Re) thermocouples are one of the most used high-temperature thermocouples for these purposes, especially for applications in vacuum or in an inert-gas atmosphere.

Recently, a number of metal–carbide–carbon fixed points have been developed for applications in radiation thermometry. Many of these fixed points, especially the Co–C (1324 °C), Ni–C (1329 °C), Pd–C (1492 °C), Pt–C (1738 °C), $Cr_7C_3-Cr_3C_2$ (1742 °C), Ru–C (1953 °C), and Ir–C (2290 °C) eutectic points and Cr_3C_2-C (1826 °C) peritectic point [1–8], are also applicable for the characterization and stability testing of W–Re thermocouples. This means that these points are not only applicable for measurements of the stability of W–Re thermocouples but also to conduct precise evaluation. Both the development of experimental apparatus of fixed points and the evaluation of thermocouples are important to realize precise temperature measurements at high temperature [3,9–12]. NMIJ has been developing the metal–carbon (M–C) eutectic-point cells and the high-temperature furnaces aiming for their application to high-temperature thermocouples. Using the developed M–C eutectic-point apparatus, the characteristics of high-temperature thermocouples have been evaluated to seek further improvement in their design and the annealing process to enhance their stability [4,12–14].

In the present study, at first, two Ru–C cells (crucible and Ru–C eutectic alloy) were constructed in our laboratory for a precise evaluation of the high-temperature thermocouples around 2000 °C. To minimize the effect due to the heat flux along the thermocouple sheath, the immersion length of the thermometer well was designed to be 116 mm. This increased immersion depth, which is aimed at a thorough evaluation of thermocouple characteristics, is a key feature of our work. More typically, miniature cells are designed for practical applications and have smaller immersion depths [6,8]. After evaluation of the melting and freezing plateaux of the constructed Ru–C cells under Ar gas, the drift of a Type C (tungsten–5 % rhenium vs tungsten–26 % rhenium) thermocouple during exposure to high temperatures around the Ru–C eutectic point was evaluated. The inhomogeneity of the Type C thermocouple was examined at 140 °C using a water heat-pipe furnace in between the drift measurements at the Ru–C eutectic point for investigation of the mechanism of the drift.

Additionally, there are also potential demands in industry for use of thermocouples under an oxidizing atmosphere at higher temperatures. However, oxidation of wires for the W–Re thermocouples can easily occur and this limits its suitability for some applications. As one possibility to solve this problem, the IrRh/Ir thermocouple is known to be applicable in an oxidizing atmosphere up to approximately 2100 °C [15]. However, to the author's knowledge, precise stability data of IrRh/Ir thermocouples using eutectic points are not reported. To investigate the stability and to explore feasibility of IrRh/Ir thermocouples at high temperature, the drift of an IrRh/Ir thermocouple (iridium–40 % rhodium vs iridium) was evaluated using another Ru–C cell.

2 Realization of Ru–C Eutectic Point

2.1 Measurement Setup of High-Temperature Furnace

To realize melting and freezing plateaux of Ru–C cells, a high-temperature furnace was employed. A schematic diagram of the high-temperature furnace is shown in Fig. 1.

The high-temperature furnace is a vertical electric furnace and consists of three-zone heaters made of carbon-fiber-reinforced carbon (C/C) composite, graphite disks, and a graphite tube as a thermometer well, in order to avoid contamination of metal components from the furnace. The furnace was filled with argon (Ar) gas flowing through gas ports during the heating. Temperature stability and uniformity with the Ru–C cell were measured using a Type C monitoring thermocouple before the drift tests were performed. This monitoring thermocouple has been exposed to 1950 °C for more than 20 h before use, and has been confirmed to be stable by checking the electromotive force (emf) three times at the Ru–C eutectic point prior to the following tests. Using this Type C monitoring thermocouple, it was found that the stability of the Ru–C cell was within 0.1 °C for over a 1 h period. The temperature distribution from the full-immersion position of the thermometer well upward to 10 cm was within 2 °C when the Ru–C alloy is all solid. Figure 2 shows a temperature profile of the high-temperature furnace. The temperature profile was measured at 1950 °C by moving a Type C monitoring thermocouple in the direction of extracting the thermocouple out from the thermometer well. As shown in Fig. 2, the temperature gradient region was approximately between 300 mm and 600 mm from the full-immersion position.
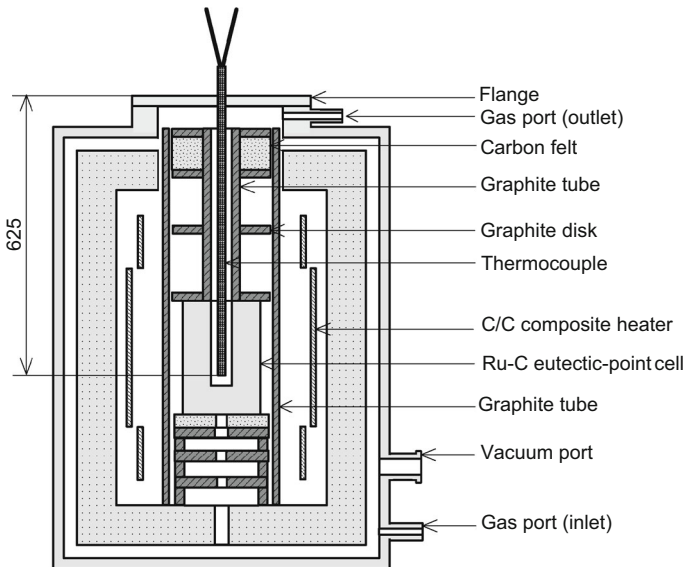

Fig. 1 Schematic diagram of high-temperature furnace
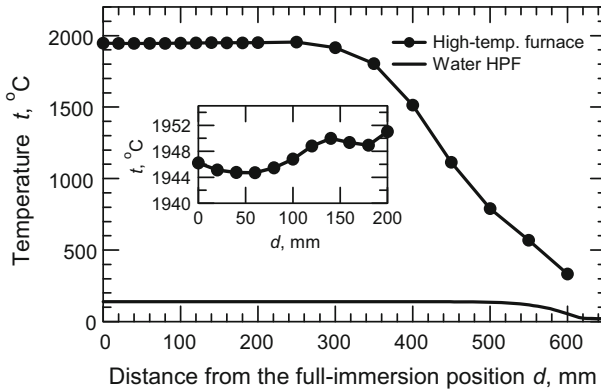
Fig. 2 Temperature profiles of high-temperature furnace containing the Ru–C cell and the water heat-pipe furnace (water HPF) used for inhomogeneity measurement

2.2 Construction of Ru–C Cell

To evaluate precisely the thermoelectric stability of W–Re thermocouples around 2000 °C, Ru–C cells were constructed in our laboratory. Figure 3 shows the dimensions of the Ru–C cells. The crucibles are made from high-purity graphite (99.9995 %, nominal value) having an outer diameter of 38 mm, and a height of 140 mm. The immersion length of the thermometer well was designed as 116 mm to minimize the effect due to the heat flux along the thermocouple sheath. All graphite crucibles were baked at 2000 °C for 3 h in vacuum before the filling of the ruthenium (Ru) powder and graphite powder. For making two Ru–C cells, graphite crucibles were filled with pure Ru powder (99.991 %, analyzed with an optical emission quantometer by the supplier) mixed with graphite powder of high purity (99.9999 %, nominal value) at approximately their eutectic composition. These cells were labeled RuC-a3 and RuC-a4. After filling, RuC-a3 and RuC-a4 contained 250 g and 231 g Ru metal, respectively.

2.3 Measurement Procedure of Ru–C Eutectic Point

To check the melting and freezing plateaux of the Ru–C cell in the high-temperature furnace before drift tests of high-temperature thermocouples, a Type C monitoring thermocouple was used. Since the thermocouple sheath is fixed on the flange, we took care that the tip of the thermocouple sheath does not contact the bottom of thermometer well to avoid breakage of the thermometer well. We insert the thermocouple before raising the furnace temperature. The tip of the sheath of the thermocouple was then adjusted to 10 mm above the bottom of the graphite well when the temperature reached around 1950 °C. The melting and freezing plateaux were induced by adjusting the setting temperature of the furnace, $T_{surround}$. We applied a stepwise setting with deviations with respect to the melting point temperature, T_{melt}. This deviation $|T_{surround} - T_{melt}|$ was held constant during the melt and freeze; however, its value was altered according to the type of thermocouple under test. According to convention,
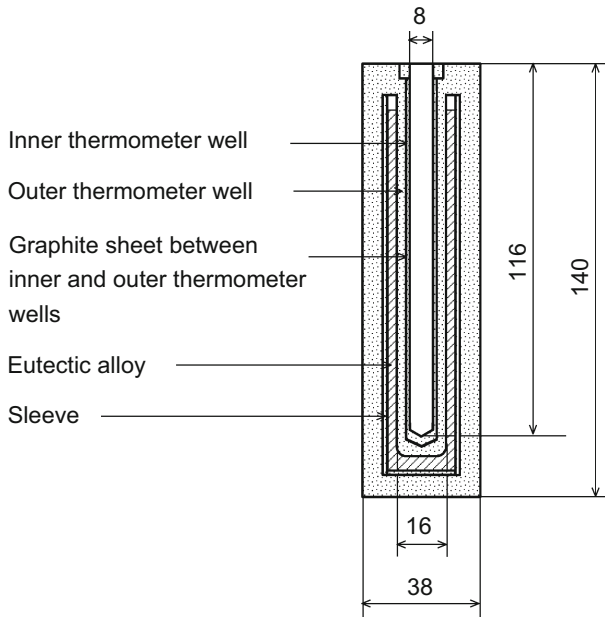
Fig. 3 Schematic diagram of the Ru–C cell

the melting point is taken as the point of inflection of the melting curve, which was obtained by a least-squares fit of a third-order polynomial function to the melting curve, while for the freezing point at the peak of the plateau soon after the supercool.

The digital multimeter used was Fluke 8508A, and the temperature of the reference junction for the measurements of drift was 0.00 °C realized using an automatically-operated ice-point device. The stability of the automatically-operated ice-point device for the reference junction of the thermocouple was estimated to be 6.5 mK (2 σ) according to our measurements.
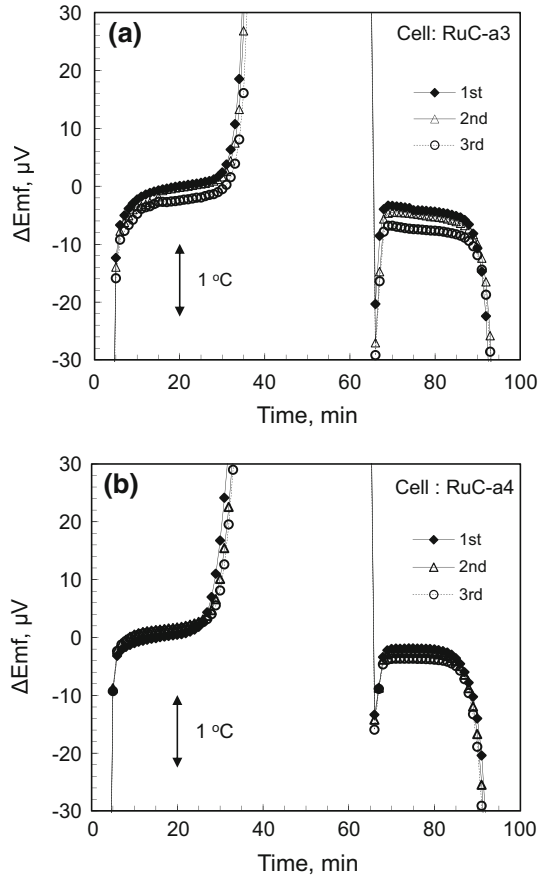
2.4 Melting and Freezing Plateaux

Before the drift tests of thermocouples, the melting and freezing plateaux of RuC-a3 and RuC-a4 were observed by means of the Type C monitoring thermocouples. Figure 4a, b shows the melting and freezing plateaux of RuC-a3 and RuC-a4, respectively. The temperature setting, $|T_{surround} - T_{melt}|$, was 16 °C. The emfs of the thermocouples at the melting and freezing points were determined as described in Sect. 2.3.

The melting and freezing plateaux of RuC-a3 were measured three times, and the standard deviation of the readings were 1.4 μV and 1.8 μV, respectively. The change of 1.4 μV in the emf of the Type C thermocouple at the Ru–C eutectic point was equivalent to 0.11 °C. The difference between the mean values of melting and freezing points was 4.1 μV, equivalent to 0.33 °C.

In a similar way, the melting and freezing points of RuC-a4 were measured three times to result in standard uncertainties of 0.8 μV and 0.9 μV, respectively. The change

Fig. 4 Typical melting and
freezing plateaux of the Ru–C
cells: (a) RuC-a3 and
(b) RuC-a4, using Type C
monitoring thermocouples

of $0.8\,\mu\text{V}$ in the emf of the Type C thermocouple at the Ru–C eutectic point was
equivalent to $0.06\,°\text{C}$. The difference between the mean values of melting and freezing
points was $3.6\,\mu\text{V}$, equivalent to $0.29\,°\text{C}$.

As shown in Fig. 4a, b, the melting and freezing plateau shapes of RuC-a3 and RuC-
a4 are satisfactory, so these cells are usable for precise drift measurements of high-
temperature thermocouples at around $1950\,°\text{C}$, described in the following sections.

3 Evaluation of W–Re Thermocouple

As in the previous section, the stability of the two newly constructed Ru–C cells
is sufficient to evaluate the characteristics of high-temperature thermocouples. By
successively realizing the plateaux of the eutectic point, we can evaluate the drift of
the emf. One interesting topic would be the drift of brand new thermocouples. So in
this study, RuC-a3 and RuC-a4 were used for drift tests of a Type C thermocouple and
an IrRh/Ir thermocouple, respectively. The information of fixed points are summarized
in Table 1 and also in the following sections.

Table 1 Characteristics of Ru–C Cells

Ru–C cell	Ru powder		Graphite crucible (%)
RuC-a3	99.991 %	250 g	99.9995
RuC-a4	99.991 %	231 g	99.9995

Table 2 Notation and characteristics of thermocouples evaluated at the Ru–C eutectic point

Thermocouple		Twin-bore insulator		Sheath		Comments
Type	Label	Material	Unit length (mm)	Material	Dimensions (mm)	
Type C	C-5	BeO	38	Ta	$\phi\,6 \times L700, t0.35$	Insulators and sheath tubes were baked at 1000 °C for 3 h in Ar gas before assembly at the manufacturer
IrRh/Ir	Ir–Rh-6	HfO$_2$	50	Ir	$\phi\,6 \times L750, t1$	–

The evaluated thermocouples were not annealed at NMIJ before the drift measurements

3.1 Construction of W–Re Thermocouples

A Type C thermocouple labeled "C-5" was prepared for the stability test at approximately 1953 °C using the Ru–C cells and the high-temperature furnace described in Sects. 2.1 and 2.2. C-5 was purchased from a manufacturer that constructed the Type C thermocouple labeled C-3 in [4]. The diameter and length of wires of C-5 were 0.5 mm and 2000 mm, respectively. Beryllia (BeO) twin-bore tubes and a tantalum (Ta) tube were used as insulators separating the wires and a thermocouple sheath, respectively, following the information in [16]. Wires were threaded through the BeO twin-bore tubes whose length was approximately 40 mm. These assemblies were inserted into the Ta tube, whose outside diameter, thickness, and length were 6 mm, 0.35 mm, and 700 mm, respectively. BeO and Ta tubes were baked in Ar gas at 1000 °C for 3 h before the thermocouple assembly was completed by the manufacturer. After the assembly, Ta tubes of C-5 were sealed to prevent the leakage of small pieces of BeO twin-bow tubes, and filled with Ar gas to avoid the oxidation of thermocouple wires. Some of the information about C-5 is summarized in Table 2 with that of the IrRh/Ir thermocouple described later in Sect. 4.1.

3.2 Measurement Setup for Inhomogeneity Measurements

Inhomogeneity of W–Re thermocouple was measured by scanning the thermocouple with a water heat-pipe furnace in between the drift measurements at the Ru–C eutectic point. Detection of even a minor emf change due to the inhomogeneity of thermocouple wires exposed at around 1950 °C requires a scanning furnace with high temperature stability. The scanning furnace must have zones of satisfactory temperature uniformity and a steep temperature gradient region, with which the inhomogeneous region of the

wires can be identified. To satisfy these conditions, a furnace containing a pressure-controlled water heat-pipe was constructed in our institute. The stability of the furnace, when working at 140 °C, was within 5 mK during 12 h which is the period for five scans of the automatic inhomogeneity tests. Details of this furnace, including a schematic diagram of the furnace, is described in [4,17].

The temperature profile of the water heat-pipe furnace is shown in Fig. 2. It is also measured by moving the Type C monitoring thermocouple at 140 °C in the same condition as that of the measurement of inhomogeneity described later. It was found that the temperature gradient region of the water heat-pipe furnace was located approximately 600 mm from the full-immersion position.

3.3 Measurement Procedure

3.3.1 Drift Measurement Procedure for Type C Thermocouple

To investigate the emf change (drift) of a Type C thermocouple around 1950 °C, emf values of C-5 were measured at the Ru–C eutectic point by using RuC-a3 in the high-temperature furnace. As already described in Sect. 2.3, the tip of the thermocouple sheath of C-5 was set apart from the bottom of the thermometer well. The tip of the sheath of C-5 was held 10 mm above the bottom of the graphite well around 1950 °C. The melting and freezing cycles of the RuC-a3 were performed every 2 h, basically following the same procedure as described in [4]. To obtain the melting and freezing plateaux of the RuC-a3, the heating and cooling patterns were applied as stepwise temperature changes. The temperature setting, $|T_{surround} - T_{melt}|$, was 16 °C. The melting and freezing cycles of RuC-a3 were repeated 112 times during the drift measurements. When interrupting to measure the inhomogeneity in between and also after finishing the drift measurements, C-5 was withdrawn from the well after the high-temperature furnace was cooled to room temperature.

3.3.2 Measurement Procedure of Inhomogeneity of Type C Thermocouple

To investigate the inhomogeneity of a thermocouple exposed at around 1950 °C, emf values of C-5 were measured at 140 °C by using the water heat-pipe furnace, where the thermocouple was moved upward at 5 mm·min^{-1} from full immersion to approximately 610 mm. At first, the inhomogeneity of C-5 was measured using the water heat-pipe furnace before the drift measurement at 1950 °C. After the drift measurement, the inhomogeneity of C-5 was measured again as the inhomogeneity post exposure at around 1950 °C for the arbitrary period, and then, the drift measurements were re-started. In this study, the inhomogeneity of C-5 was measured 15 times.

The emf of the thermocouple was measured automatically using a digital multimeter (Wavetek/Datron 1281). The reference junction of the thermocouple was maintained at 0 °C using crushed ice. Although the measured emf includes the emf due to ambient temperature and the reference junction, its fluctuation is negligible since the room temperature is stable.
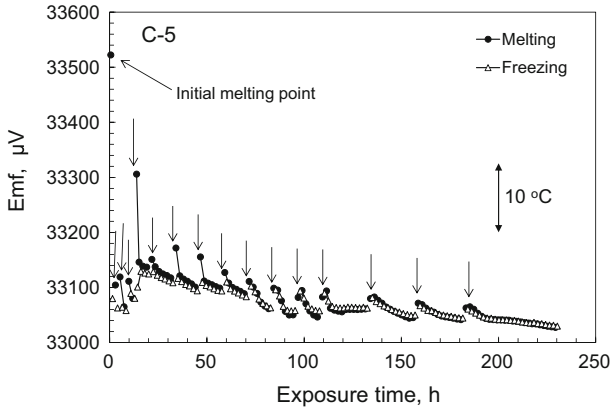
Fig. 5 Emfs of C-5 measured at the melting and freezing points of Ru–C cell, RuC-a3

3.4 Observation of Drift and Inhomogeneity of Type C Thermocouple

3.4.1 Drift of Type C Thermocouple at Ru–C Eutectic Point

Figure 5 shows emf changes (drifts) of C-5. The position of the measuring junction of the thermocouple during the measurements was fixed at the full-immersion position $d = 0$ mm, as shown in Fig. 1. The ordinate shows the emfs of C-5, while the abscissa shows the exposure time at around 1950 °C. Closed circles and open triangles indicate the emfs at the melting and freezing points of RuC-a3, respectively. Down arrows in Fig. 5 indicate that C-5 was withdrawn after cooling the high-temperature furnace to room temperature, which interrupted the drift measurements. As shown in Fig. 5, the initial emf value at the melting point after 1 h exposure was 33 522.2 µV, and then, the emf value at the freezing point after 2 h exposure was 33 079.8 µV. The emf of C-5 decreased about 442 µV (35 °C) within the first 2 h exposure at around 1950 °C. This difference between the emfs for melting and freezing is significant; however, a similar change for Type C thermocouples at the Ru–C eutectic point has been also reported in [6]. The emf change of C-5 in the exposure time from 5 h to 15 h was approximately 70 µV (5.6 °C). After 15 h exposure, the emf of C-5 decreased gradually. The emf difference of C-5 between 15 h and 230 h exposures was 100 µV (8.0 °C).

To check the reproducibility of the melting and freezing temperatures of RuC-a3 during the drift measurement, a comparison of the emf at melting and freezing temperatures before and after the drift measurement was conducted using the Type C monitoring thermocouple. Since the emfs measured before and after the drift measurement agreed within 3.7 µV (equivalent to 0.3 °C) at the melting point and 10.6 µV (equivalent to 0.8 °C) at the freezing point, respectively, it is considered that the emf changes shown in Fig. 5 indicate the drifts of C-5.

3.4.2 Inhomogeneity of Type C Thermocouple Measured at 140 °C

The thermoelectric inhomogeneity characteristics were measured using the water heat-pipe furnace during the measurement of the emf drift at the Ru–C eutectic point. The
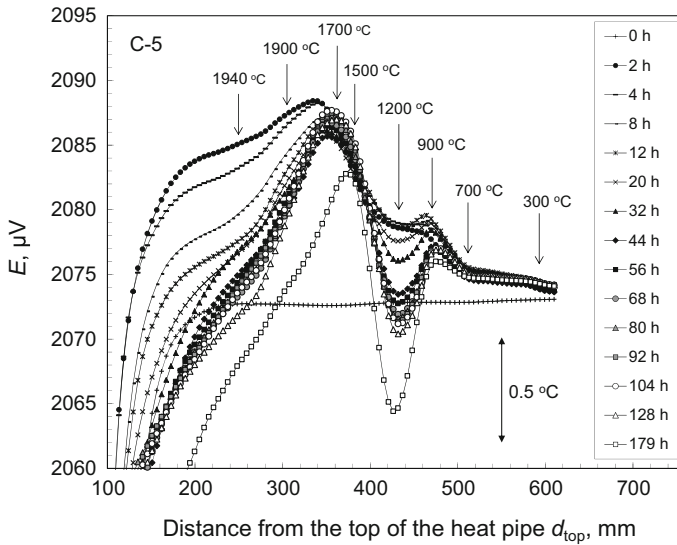
Fig. 6 Emf changes of C-5 measured at 140 °C by scanning the thermocouple within a water heat-pipe furnace during the drift measurement at the Ru–C eutectic point

inhomogeneity of C-5 was measured at the "as received condition" (0 h exposure) and at the intermediate condition (from 2 h to 179 h exposures). At the end of the drift measurements (231 h exposure), an inhomogeneity measurement was not possible since the Ta sheath of C-5 was slightly bent due to exposure at around 1950 °C for a long period for the drift test.

The inhomogeneity tests were performed five times at each exposure time. For each scan, the inhomogeneity was measured by dragging the thermocouple out of the furnace. No obvious change was observed among the five scans within the same inhomogeneity test. Figure 6 shows the mean emf values of C-5 at 140 °C, using the water heat-pipe furnace, as a function of distance from the top of the heat pipe, d_{top}. When the tip of the test thermocouple is inserted at the full-immersion position, $d_{top} =$ 610 mm, the gradient region of the heat-pipe furnace was located at approximately 610 mm from the tip of the test thermocouple [17]. This means that the emf generated in the thermocouple wires at around 610 mm from the tip of the test thermocouple is observed when the tip of the test thermocouple is at the full-immersion position, $d_{top} = 610$ mm. According to a relationship between d_{top} and the temperature profile of the high-temperature furnace shown in Fig. 1, the exposure temperatures can be obtained. The exposure temperatures are indicated in Fig. 6 with down arrows.

As shown in Fig. 6, it is obvious that the inhomogeneity vastly increased within the first 2 h exposure. The inhomogeneity below $d_{top} = 500$ mm has increased especially significantly. In other words, the inhomogeneity of the locations exposed above approximately 700 °C increased significantly within the first 2 h exposure. This emf change is considered to be mainly caused by grain growth in the W-rich wire (W5Re) of the Type C thermocouple [18].
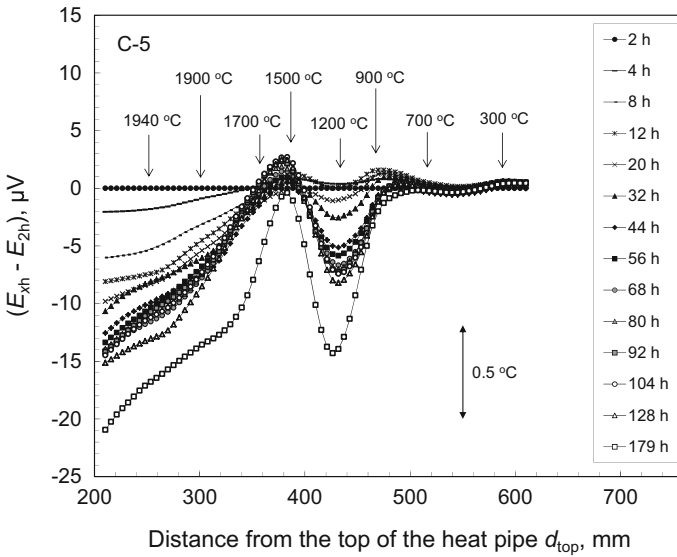
Fig. 7 Emf difference, $E_{xh} - E_{2h}$, between the emf values at 2 h exposure, E_{2h}, and at x h exposure, E_{xh}, of C-5 measured at 140 °C using the water heat-pipe furnace during the drift measurement at the Ru–C eutectic point

In order to clarify further emf changes of C-5 beyond 2 h exposure, the emf difference, $E_{xh} - E_{2h}$, where E_{2h} is the emf after 2 h exposure, and E_{xh} being that after x h exposure, is calculated and shown in Fig. 7. The ordinate in Fig. 7 shows $E_{xh} - E_{2h}$, while the abscissa shows the distance, d_{top}, from the top of the water heat pipe. The exposure temperatures are indicated with arrows. It was found that $E_{xh} - E_{2h}$ around 1200 °C and above 1500 °C decreased gradually after exposure. This result around 1200 °C agrees with that obtained from C-3 in [4]. As described in [4], to explain these emf changes, there are several possibilities. Burns et al. [18] examined the drift of the Type D (W–3 % Re vs W–25 % Re) thermocouple around 2000 °C and reported the preferential loss of Re from the thermoelements of W–25 % Re. Rempe et al. [19] investigated the drift of Type C at 1500 °C, and reported the impact of precipitate formation due to material phase changes on the thermoelectric response. At the present state, the mechanism of this emf change is not clear, but considering the findings reported in [18,19] explaining the phenomenon related to Re within the thermoelectric wire, we speculate that the emf change observed in our measurements may also have been related to the Re-rich wire (W–26 % Re).

4 Application to IrRh/Ir Thermocouple

4.1 Preparation of IrRh/Ir Thermocouples

The IrRh/Ir thermocouple is known to be applicable up to approximately 2100 °C [15]. To investigate the stability and to explore the feasibility of the IrRh/Ir thermocouple

at high temperature, the IrRh/Ir thermocouple labeled "Ir-Rh-6" was prepared. The diameter and length of wires of Ir–Rh-6 used were 0.5 mm and 2000 mm, respectively. Hafnia (HfO$_2$) twin-bore tubes were used as insulators separating the wires. The wires were threaded through the HfO$_2$ twin-bore tubes whose length was approximately 50 mm. These assemblies were inserted into the iridium (Ir) tube, whose outside diameter, thickness, and length were 6 mm, 1 mm, and 750 mm, respectively, instead of a Ta tube to avoid the breakage of thermocouple wires, since a chemical reaction occurs between Ir and Ta metals at approximately 1950 °C [20].

The emf change (drift) of Ir–Rh-6 around 1950 °C was measured at the Ru–C eutectic point by using RuC-a4 in the high-temperature furnace, except during an interruption for inhomogeneity measurements. The melting and freezing cycles of the Ru–C cell were performed every 4 h under the temperature setting, $|T_{\text{surround}} - T_{\text{melt}}|$ of 8 °C. The melting and freezing cycles of RuC-a4 were repeated 13 times during the drift measurements.

4.2 Drift of IrRh/Ir Thermocouples at Ru–C Eutectic Point

During the drift measurements of Ir–Rh-6 using RuC-a4 in the high-temperature furnace, the position of the measuring junction of Ir–Rh-6 was fixed at the full-immersion position $d = 0$ mm during the measurements.

Figure 8 shows the emf changes (drifts) of Ir–Rh-6. The ordinate shows the emfs of Ir–Rh-6, while the abscissa shows the exposure time at around 1950 °C. Closed circles and open triangles indicate the emfs at the melting and freezing points of RuC-a4, respectively. Such an initial large emf change reported for C-5 in Fig. 5 did not appear immediately after exposure for IrRh/Ir. The emf of Ir–Rh-6 at the melting point increased gradually, while that at the freezing point showed an almost constant value for the first 40 h after exposure. It was found that the emf changes of Ir–Rh-6 at the
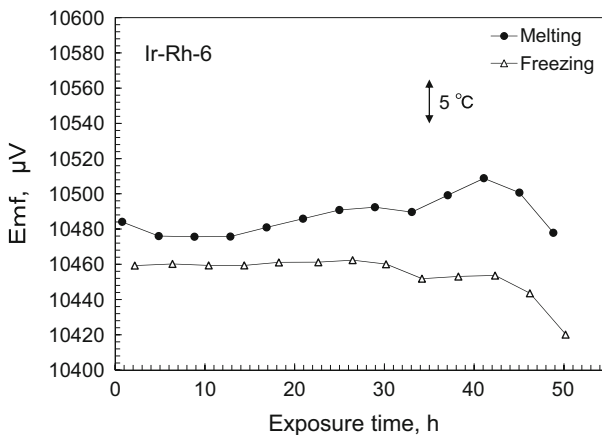

Fig. 8 Emfs of Ir–Rh-6 measured at the melting and freezing points of Ru–C cell, RuC-a4

melting and freezing points were approximately 30 µV (5.5 °C) and 10 µV (1.9 °C), respectively, within the first 40 h exposure.

To check the reproducibility of the melting and freezing temperatures of RuC-a4 during the drift measurement, the comparison of the emfs at melting and freezing temperatures, before and after the drift measurement, was conducted using the Type C monitoring thermocouple. Since the emfs measured before and after the drift measurement agreed within 1.7 µV (equivalent to 0.1 °C) and 2.0 µV (equivalent to 0.2 °C) at the melting and freezing points, respectively, we consider that the emf changes shown in Fig. 8 indicate the drifts of Ir–Rh-6.

This result implies that the Ru–C cell is also useful for the evaluation of drift of high-temperature thermocouples, and its application is not limited to W–Re thermocouples.

5 Conclusion

NMIJ, AIST has been developing M–C eutectic-point cells and high-temperature furnaces aiming for their application to high-temperature thermocouples. Using the developed M–C eutectic-point apparatus, the characteristics of high-temperature thermocouples has been evaluated to seek further improvement. In this study, two Ru–C cells for thermocouple calibration were constructed. The cells showed good melting and freezing plateaux by means of a Type C thermocouple. The emf of the Type C thermocouple, C-5, at around 1953 °C decreased rapidly within the first 2 h, and after that, the emf tended to decrease gradually. The emf of C-5 measured at 140 °C aimed for determining the inhomogeneity effect on the emf using the heat-pipe furnace showed large emf changes due to the exposure around 1200 °C and that above around 1500 °C in the high-temperature furnace.

In addition, to investigate a possible application of another type of high-temperature thermocouples, the drift of the IrRh/Ir thermocouple, Ir–Rh-6, was evaluated. It was found that the emf of Ir–Rh-6 at the melting point of Ru–C cell tended to increase gradually for the first 40 h exposure and then decrease.

Since this report is at the early stage of our ongoing project to seek the feasibility of the Ru–C eutectic point to calibrate high-temperature thermocouples, one Type C thermocouple and one IrRh/Ir thermocouple were used to investigate the drift and inhomogeneity. Nevertheless, these experimental results show that the Ru–C eutectic point is useful to investigate accurately the drift of high-temperature thermocouples. The evaluation of drift and inhomogeneity is important for an accurate thermocouple calibration. The results obtained in this study will be useful for evaluating the uncertainty of thermocouple calibration at around 2000 °C.

References

1. R. Morice, M. Megharfi, J.O. Favreau, E. Morel, I. Didialaoui, J.R. Filtz, in *Proceedings of TEMP-MEKO 2004, 9th International Symposium on Temperature and Thermal Measurements in Industry*

and Science, ed. by D. Zvizdić, L.G. Bermanec, T. Veliki, T. Stašić (FSB/LPM, Zagreb, Croatia, 2004), pp. 847–852

2. Y.G. Kim, I. Yang, in *Proceedings XVIII IMEKO World Congress* (IMEKO, Rio de Janeiro, Brazil, 2006)
3. H. Ogura, T. Deuze, R. Morice, P. Ridoux, J.R. Filtz, SICE J. Control Meas. Syst. Integr. **3**, 081 (2010)
4. H. Ogura, M. Izuchi, M. Arai, Int. J. Thermophys. **32**, 2420 (2011)
5. O. Ongrai, J.V. Pearce, G. Machin, S.J. Sweeney, Meas. Sci. Technol. **22**, 105103 (2011)
6. O. Ongrai, J.V. Pearce, G. Machin, S.J. Sweeney, in *Proceedings of Ninth International Temperature Symposium* (Los Angeles), *Temperature: Its Measurement and Control in Science and Industry*, vol. 8, ed. by C.W. Meyer, AIP Conference Proceedings 1552 (AIP, Melville, NY, 2013), pp. 504–509
7. M. Gotoh, in *Proceedings of Ninth International Temperature Symposium* (Los Angeles), *Temperature: Its Measurement and Control in Science and Industry*, vol. 8, ed. by C.W. Meyer, AIP Conference Proceedings 1552 (AIP, Melville, NY, 2013), pp. 587–590
8. J.V. Pearce, C.J. Elliott, G. Machin, O. Ongrai, in *Proceedings of Ninth International Temperature Symposium* (Los Angeles), *Temperature: Its Measurement and Control in Science and Industry*, vol. 8, ed. by C.W. Meyer, AIP Conference Proceedings 1552 (AIP, Melville, NY, 2013), pp. 595–599
9. Y. Yamada, H. Sakate, A. Ono, Metrologia **37**, 71 (2000)
10. H. Ogura, M. Izuchi, M. Arai, Int. J. Thermophys. **29**, 210 (2008)
11. H. Ogura, M. Izuchi, J. Tamba, M. Arai, in *Proceedings ICROS-SICE International Joint Conference 2009* (SICE, Tokyo, 2009), pp. 3297–3302
12. J.V. Pearce, H. Ogura, M. Izuchi, G. Machin, Metrologia **46**, 473 (2009)
13. H. Ogura, K. Yamazawa, M. Izuchi, M. Arai, in *Proceedings of TEMPMEKO 2004, 9th International Symposium on Temperature and Thermal Measurements in Industry and Science*, ed. by D. Zvizdić, L.G. Bermanec, T. Veliki, T. Stašić (FSB/LPM, Zagreb, Croatia, 2004), pp. 459–464
14. H. Ogura, M. Izuchi, J. Tamba, M. Arai, in *Proceedings of Ninth International Temperature Symposium* (Los Angeles), *Temperature: Its Measurement and Control in Science and Industry*, vol. 8, ed. by C.W. Meyer, AIP Conference Proceedings 1552 (AIP, Melville, NY, 2013), pp. 554–559
15. ASTM E1751/E1751M-09el, Standard Guide for Temperature Electromotive Force (emf) Tables for Non-letter Designated Thermocouple Combinations (ASTM International, West Conshohocken, PA, 2009)
16. R. Morice, J.O. Favreau, T. Deuze, J.R. Filtz, in *Proceedings SICE 2005* (SICE, Tokyo, 2005), pp. 678–682
17. J. Tamba, K. Yamazawa, S. Masuyama, H. Ogura, M. Izuchi, Int. J. Thermophys. **32**, 2436 (2011)
18. G.W. Burns, W.S. Hurst, in *Temperature: Its Measurement and Control in Science and Industry*, vol. 4, Part 3, authored by H.H. Plumb, ed. by H. Harmon, D.I. Finch, G.W. Burns, R.L. Berger, T.E. Van Zandt (ISA, Pittsburgh, PA, 1972), pp. 1751–1766
19. J.L. Rempe, D.L. Knudson, J.E. Daw, S.C. Wilkins, Meas. Sci. Technol. **19**, 115201 (2008)
20. T.B. Massalski, H. Okamoto, P.R. Subramanian, L. Kacprzak (eds.), in *Binary Alloy Phase Diagrams*, 2nd edn. (ASM International, Materials Park, OH, 1990), p. 2355